THE DYNAMIC PROPERTY AND CHAOS CONTROL FOR A TWO-DEGREE-OF-FREEDOM VIBRO-IMPACT SYSTEM

Guo FENG[1], Pan JIAN-XUN[1], Mu YONG[1], Ji ZHEN-DONG[1]

The dynamic behavior of a two-degree-of-freedom vibro-impact system is studied in this paper. It is shown that there exist Hopf bifurcations in the vibro-impact systems with two or more degrees of freedom under suitable parameters. A center manifold theorem technique is applied to reduce the Poincaré mapping of the vibro-impact system to a two-dimensional one, and then the theory of Hopf bifurcation of maps in R^2 is applied to conclude the existence of Hopf bifurcation of the vibro-impact system. The quasi-periodic response of the system, which represented by invariant circles in the projected Poincaré section, is obtained by numerical simulations, and the routes of quasi-periodic impacts to chaos are stated briefly. In this paper, a control parameter is selected. Through the improvement of OGY control method and using the pole placement technique of the linear control theory, the chaotic motion of the vibro-impact system is controlled to an unstable period-1 or period-2 orbit. At the same time, the different choice of the regulator poles is analyzed. By numerical simulation, the effectiveness of the method is demonstrated.

Keywords: Vibro-impact system; Hopf bifurcation; OGY chaos control; Pole placement

1. Introduction

Vibro-impact system is widely applied in the practical engineering fields [1-4]. Many engineers and scientists pay increasing attention to the complexity of the dynamics. For multi-degree-of-freedom vibro-impact system (a class of higher-dimensional strongly nonlinear dynamic systems), [5-9] studied a variety of bifurcation, symmetry and chaos of such systems by applying the center manifold theorem and numerical simulations.

Chaos exists in mechanics, physics, chemistry, biology, geography and even the social sciences widely. How to use and control chaos has become one of the hottest fields of the basic research in natural sciences. At present, a lot of chaos control methods, such as the way of feedback control with external excitation or damping [10], have actually changed the dynamical properties of the

[1] Department of Basic, Shandong Women's University, Jinan 250300, China;
Email: sdwugf@163.com

original system, because of a large control element added.

In 1990, Ott, Grebogi and Yorke [11] proposed a method of chaos control which is called OGY method. The advantage of the method is only a very small control signal will control the dynamic behavior of the system to an unstable periodic orbit, or to obtain mutual transformation between different unstable periodic orbits in chaotic attractors.

Since then, many scholars [12–17] presented many improvement methods according to different situations. The OGY method was obtained the further development. Ott, Grebogi, Romeiras and Dayawansa [20] improved the OGY method using the pole placement technique of the linear control system. About the improvement of the OGY method, the chaos control of the high period in chaotic attractors and the high dimensional systems is an important trend.

As a class of typical nonlinear dynamical systems of the actual engineering, vibro-impact systems will appear chaos phenomena inevitably. Souza de et al has applied OGY chaos control method to a class of one-degree-of-freedom vibrato-impact system [21, 22]. Because the Poincaré impact mapping of one-degree-of-freedom of vibrato-impact system is a two-dimensional mapping, it is easy to apply the method to control the chaotic behavior of it. However, the multi-degree-of-freedom vibro-impact systems exist in the actual engineering fields frequently. How to study the multi-degree-of-freedom vibro-impact systems by the OGY chaos control method becomes very important and necessary. In this paper, through the improvement of OGY [20], we study the chaos control of a two-degree-of-freedom vibro-impact system [5]. By establishing linear mapping and using the pole placement technique of the linear control theory, we determine the controllable matrix and select the appropriate poles, which depends on the control parameter. The chaotic behavior of the system is controlled effectively. Because of the different selection of the pole values and the range size of the disturbance parameters, the average time of the control is analyzed. The result shows that OGY chaos control method can be applied to the multi-degree-of-freedom vibro-impact systems and high-dimensional systems.

2. Mechanics Model and the Motion Equation of Vibro-impact System

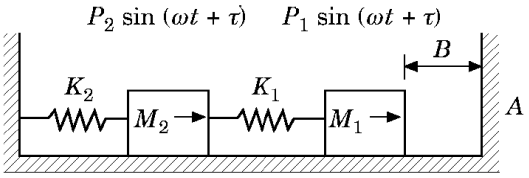

Fig. 1. A schematic of the two-degree-freedom impact oscillator

The mechanical model for a two-degree-of-freedom vibrator with masses

M_1 and M_2 is shown in Fig. 1. The masses are connected to linear springs with stiffness K_1 and K_2. The excitations on both masses are harmonic with amplitudes P_1 and P_2. The mass M_1 impacts against a rigid surface when its displacement X_1 equals the gap B. The impact is described by a coefficient of restitution R, and it is assumed that the duration of impact is negligible compared to the period of the force. It is assumed that the horizontal support surface is smooth.

Between impacts, the differential equations of motion are

$$\begin{bmatrix} M_1 & 0 \\ 0 & M_2 \end{bmatrix} \frac{d^2}{dT^2} \begin{Bmatrix} X_1 \\ X_2 \end{Bmatrix} + \begin{bmatrix} K_1 & -K_1 \\ -K_1 & K_1 + K_2 \end{bmatrix} \begin{Bmatrix} X_1 \\ X_2 \end{Bmatrix} = \begin{Bmatrix} P_1 \\ P_2 \end{Bmatrix} \sin(\Omega T + \tau) \tag{1}$$

The impact equation of mass M_1 is

$$\dot{X}_{1+} = -R\dot{X}_{1-} \tag{2}$$

Where $\dot{X}_{1+} = -R\dot{X}_{1-}$ and X_{1-} represent the impacting mass velocities of approach and departure respectively. For convenience, the equations of motion (1) are rewritten in non-dimensional form for $x_1 < B$, as

$$\left\{ \begin{bmatrix} 1 & 0 \\ 0 & \mu_m \end{bmatrix} \begin{Bmatrix} \ddot{x}_1 \\ \ddot{x}_2 \end{Bmatrix} + \begin{bmatrix} 1 & -1 \\ -1 & 1+\mu_k \end{bmatrix} \begin{Bmatrix} x_1 \\ x_2 \end{Bmatrix} = \begin{Bmatrix} 1-f_2 \\ f_2 \end{Bmatrix} \sin(\omega t + \tau) \right. \tag{3}$$

Where the non-dimensional quantities

$$\mu_m = \frac{M_2}{M_1},\ \mu_K = \frac{K_2}{K_1},\ f_2 = \frac{P_2}{P_1 + P_2},\ \omega = \Omega\sqrt{\frac{M_1}{K_1}},\ t = T\sqrt{\frac{K_1}{M_1}},\ b = \frac{BK_1}{P_1 + P_2},\ x_i = \frac{X_i K_1}{P_1 + P_2} \tag{4}$$

3. The Period Motion Analysis of the System

The equations of motion (3) are resolved by using the formal co-ordinate and modal matrix approach. The general solution of equation (3) takes the form

$$x_i = \sum_{j=1}^{2} \psi_{ij} \left(a_j \cos \omega_j t + b_j \sin \omega_j t + A_j \sin(\omega t + \tau) \right) \tag{5}$$

$$\dot{x}_i = \sum_{j=1}^{2} \psi_{ij} \left(-a_j \omega_j \sin \omega_j t + b_j \omega_j \cos \omega_j t + A_j \omega \cos(\omega t + \tau) \right) \quad (i = 1, 2) \tag{6}$$

Where ψ_{ij} are elements of the canonical modal matrix ψ, A_j are the amplitude parameters and $A_j = \psi_j^T P / \left(\omega_j^2 - \omega^2 \right), P = (1 - f_2,\ f_2)$, a_j and b_j are the constants of integration, which are determined by the initial conditions and modal parameters of the system.

Under suitable system parameter conditions, the vibro-impact system given in Figure 1 can exhibit periodic behavior. The periodic behavior means that if the dimensionless time t is set to zero directly after an impact, it becomes

$t = 2\pi/\omega$ just before the next impact.

$$x_1(0) = b,\ x_1(2\pi/\omega) = b,\ \dot{x}_{1+}(0) = -R\dot{x}_{1-}(0),\ x_2(0) = x_2(2\pi/\omega),\ \dot{x}_2(0) = \dot{x}_2(2\pi/\omega) \quad (7)$$

The first and second equations express the instantaneous nature of each impact, the third equation is the impact law, and the fourth and fifth equations express the continuity of position and velocity of mass M_2 at the instant of impact. Inserting the equation (7) into the equation (3), we can solve for the constants a_j and b_j of integration and the phase angle τ_0 from equations (5) and (6) and express them as set out below.

If b= 0, then let $\tau_0 = \bar{\tau}_0$:

$$\bar{\tau}_0 = \tan^{-1}\left(\frac{\left(\psi_{22}\psi_{11}s_1(1-c_2)\omega_2 - \psi_{12}\psi_{21}s_2(1-c_1)\omega_1\right)(1+R)\omega}{D\omega_1\omega_2(1-c_1)(1-c_2)(1-R)}\right) \quad (8)$$

$$\tau_0 = \cos^{-1}\left(\frac{b\tan\bar{\tau}_0 \pm \sqrt{\left(\tan^2\bar{\tau}_0 + 1\right)d^2 - b^2}}{\left(\tan^2\bar{\tau}_0 + 1\right)d}\right) \quad (9)$$

$$b_1 = \frac{d\psi_{22}(1+R)\omega\cos\tau_0}{D\omega_1(1-R)},\ b_2 = -\frac{\psi_{21}\omega_1 b_1}{\psi_{22}\omega_2},\ a_i = \frac{b_i s_i}{1-c_i},\ (i = 1,2) \quad (10)$$

Where $s_i = \sin 2\pi\omega_i/\omega$, $c_i = \cos 2\pi\omega_i/\omega$, $d = -(\psi_{11}A_1 + \psi_{12}A_2)$, $D = |\psi|$.

Otherwise, it is impossible for periodic impacts to exist. Substituting equations (8)–(10) into the general solutions of equation (3), we obtain the periodic solutions of the system shown in Figure 1, which correspond to one impact during one cycle of the forcing:

$$x_i = \sum_{j=1}^{2}\psi_{ij}\left(a_j\cos\omega_j t + b_j\sin\omega_j t + A_j\sin(\omega t + \tau_0)\right) \quad (t \bmod 2\pi/\omega) \quad (11)$$

$$\dot{x}_i = \sum_{j=1}^{2}\psi_{ij}\left(-a_j\omega_j\sin\omega_j t + b_j\omega_j\cos\omega_j t + A_j\omega\cos(\omega t + \tau_0)\right) \quad (t \bmod 2\pi/\omega) \quad (12)$$

4. Poincaré Mapping and the Stability of Periodic Motion

Take the collision surface $\sigma \subset R^4 \times S$ as the Poincaré section. Let $\sigma = \left\{(x_1, \dot{x}_1, x_2, \dot{x}_2, \theta) \in R^4 \times S,\ x_1 = b\right\}$, let us consider the perturbed motion. For $\tilde{x}_1 \le b$, the solutions of the perturbed motion are written in the form

$$\tilde{x}_i = \sum_{j=1}^{2} \psi_{ij} \left(\tilde{a}_j \cos \omega_j t + \tilde{b}_j \sin \omega_j t + A_j \sin(\omega t + \tau_0 + \Delta\tau) \right) \tag{13}$$

$$\dot{\tilde{x}}_i = \sum_{j=1}^{2} \psi_{ij} \left(-\tilde{a}_j \omega_j \sin \omega_j t + \tilde{b}_j \omega_j \cos \omega_j t + A_j \omega \cos(\omega t + \tau_0 + \Delta\tau) \right) \tag{14}$$

The integration constants $\tilde{a}_1, \tilde{a}_2, \tilde{b}_1, \tilde{b}_2$. Dimensionless time after the collision is zero, and the next time of before the collision is $t = (2\pi + \Delta\theta)/\omega$. Let $t_e = (2\pi + \Delta\theta)/\omega$, so that $\sum_{i=1}^{2} \psi_{1i} \tilde{\xi}_i (t_e) = b.$ Let

$$g(\ \Delta\dot{x}_{10}, \Delta x_{20}, \Delta\dot{x}_{20}, \Delta\tau, \Delta\theta) = \sum_{i=1}^{2} \psi_{1i} \tilde{\xi}_i (t_e) - b \tag{15}$$

Where

$$\tilde{\xi}_i (t) = \tilde{a}_i \cos \omega_i t + \tilde{b}_i \sin \omega_i t + A_i \sin(\omega t + \tau_0 + \Delta\tau),$$

$$\dot{\tilde{\xi}} (t)_i = -\tilde{a}_i \omega_i \sin \omega_i t + \tilde{b}_i \omega_i \cos \omega_i t + A_i \omega \cos(\omega t + \tau_0 + \Delta\tau).$$

The conditions under which there exist fixed points give

$$g(\ \Delta\dot{x}_{10}, \Delta x_{20}, \Delta\dot{x}_{20}, \Delta\tau, \Delta\theta)\big|_{(0,0,0,0,0)} = 0.$$

According to the implicit function theorem, the equation (15) can be solved as

$$\Delta\theta = \Delta\theta(\ \Delta\dot{x}_{10}, \Delta x_{20}, \Delta\dot{x}_{20}, \Delta\tau), \Delta\theta(\ 0,0,0,0) = 0 \tag{16}$$

We finally obtain the Poincaré mapping

$$\begin{aligned}
\Delta\dot{x}'_{10} &= \tilde{f}_1(\ \Delta\dot{x}_{10}, \Delta x_{20}, \Delta\dot{x}_{20}, \Delta\tau, \Delta\theta) - \Delta\dot{x}_{10} \overset{def}{=} f_1(\ \Delta\dot{x}_{10}, \Delta x_{20}, \Delta\dot{x}_{20}, \Delta\tau), \\
\Delta x'_{20} &= \tilde{f}_2(\ \Delta\dot{x}_{10}, \Delta x_{20}, \Delta\dot{x}_{20}, \Delta\tau, \Delta\theta) - \Delta x_{20} \overset{def}{=} f_2(\ \Delta\dot{x}_{10}, \Delta x_{20}, \Delta\dot{x}_{20}, \Delta\tau), \\
\Delta\dot{x}'_{20} &= \tilde{f}_2(\ \Delta\dot{x}_{10}, \Delta x_{20}, \Delta\dot{x}_{20}, \Delta\tau, \Delta\theta) - \Delta\dot{x}_{20} \overset{def}{=} f_3(\ \Delta\dot{x}_{10}, \Delta x_{20}, \Delta\dot{x}_{20}, \Delta\tau), \\
\Delta\tau' &= \tilde{f}_4\left(\Delta\tau + \Delta\theta(\ \Delta\dot{x}_{10}, \Delta x_{20}, \Delta\dot{x}_{20}, \Delta\tau)\right) \overset{def}{=} f_4(\ \Delta\dot{x}_{10}, \Delta x_{20}, \Delta\dot{x}_{20}, \Delta\tau)
\end{aligned} \tag{17}$$

The Poincaré map (17) can be expressed as

$$\Delta X' = f(\omega, \Delta X) \tag{18}$$

In which

$$\Delta X = \left(\Delta\dot{x}_{10}, \Delta x_{20}, \Delta\dot{x}_{20}, \Delta\tau\right)^{\mathrm{T}},\ \Delta X' = \left(\Delta\dot{x}'_{10}, \Delta x'_{20}, \Delta\dot{x}'_{20}, \Delta\tau'\right)^{\mathrm{T}},$$

$$f\left(\omega, \Delta X\right) = \left(f_1, f_2, f_3, f_4\right)^{\mathrm{T}}.$$

Linearizing the Poincare´ map at the fixed point results in the matrix

$$Df\left(\omega, 0\right) = \left[\begin{array}{cccc} \dfrac{\partial f_1}{\partial\Delta\dot{x}_{10}} & \dfrac{\partial f_1}{\partial\,\Delta x_{20}} & \dfrac{\partial f_1}{\partial\Delta\dot{x}_{20}} & \dfrac{\partial f_1}{\partial\Delta\tau} \\ \dfrac{\partial f_2}{\partial\Delta\dot{x}_{10}} & \dfrac{\partial f_2}{\partial\,\Delta x_{20}} & \dfrac{\partial f_2}{\partial\Delta\dot{x}_{20}} & \dfrac{\partial f_2}{\partial\Delta\tau} \\ \dfrac{\partial f_3}{\partial\Delta\dot{x}_{10}} & \dfrac{\partial f_3}{\partial\,\Delta x_{20}} & \dfrac{\partial f_3}{\partial\Delta\dot{x}_{20}} & \dfrac{\partial f_3}{\partial\Delta\tau} \\ \dfrac{\partial f_4}{\partial\Delta\dot{x}_{10}} & \dfrac{\partial f_4}{\partial\,\Delta x_{20}} & \dfrac{\partial f_4}{\partial\Delta\dot{x}_{20}} & \dfrac{\partial f_4}{\partial\Delta\tau} \end{array}\right]_{(v,0,0,0,0)}.$$

Let $\Delta X = \left(\Delta\dot{x}_{10}, \Delta x_{20}, \Delta\dot{x}_{20}, \Delta\tau\right)^{\mathrm{T}}$ denote $\Delta X = \left(\Delta x_1, \Delta x_2, \Delta x_3, \Delta x_4\right)^{\mathrm{T}}$. By the implicit function theorem, it is easy to calculate the following derivatives in matrix

$$\frac{\partial\Delta\theta}{\partial\Delta x_i} = -\frac{\partial G}{\partial\Delta x_i}\Big/\frac{\partial G}{\partial\Delta\theta},\ \left(i = 1, 2, 3, 4\right) \tag{19}$$

$$\frac{\partial f_i}{\partial\Delta x_i} = \frac{\partial\tilde{f}_i}{\partial\Delta x_i} + \frac{\partial\tilde{f}_i}{\partial\Delta\theta}\cdot\frac{\Delta\theta}{\partial\Delta x_i},\ \left(i = 1, 2, 3, 4\right) \tag{20}$$

The eigenvalues of *Df*(*v*, 0) can be obtained in fixed point. If all eigenvalues of *Df*(*v*, 0) are inside the unit circle, then the periodic solution is stable; otherwise, it is unstable. When the eigenvalues of *Df*(*v*, 0) with the largest modules are on the unit circle, bifurcations occur in various ways according to their numbers and their positions on the unit circle, resulting in qualitative changes in the system dynamics. When the system is disturbed a little, the unstable fixed point of the map will become quasi-periodic solutions. Mapping indicates Hopf bifurcation in fixed point, even though the continuous bifurcation may lead to chaos.

5. The Chaos Control of High-dimensional Systems by OGY Method

The main idea of this method is that one of the unstable periodic orbits embedded in the attractors is chosen as a control target. When the chaotic motion wanders into the vicinity of the periodic motion, a certain parameter of the system is perturbed. The pole and the controllable matrix is determined correctly by the

pole placement technique of the linear control systems [23]. Then the chaotic motion will stabilize to the periodic motion.

Consider the following map:

$$\boldsymbol{Z}_{i+1}=\boldsymbol{F}\left(\boldsymbol{Z}_i, a\right), \boldsymbol{Z}_i \in \square^2, a \in \square \tag{21}$$

F is sufficiently smooth, and the parameter a is the adjustable parameter which is restricted to lie in the small interval $|a-\bar{a}|<\delta$. $\bar{a}$ is a nominal value. There exists a chaotic attractor of the system as $a=\bar{a}$. The unstable periodic motion will be the control target now. The system parameter a is perturbed timely, such that the chaotic motion converges to the expected periodic orbit in the attractor. Ergodic nature of the chaos dynamics ensures that the state trajectories eventually enter into the neighborhood of the stable periodic orbits. Once inside, then the stabilizing feedback control law is applied in order to control the trajectory to the desired periodic orbit.

If $\boldsymbol{Z}_*(\bar{a})$ is an unstable fixed point of the map (21), then the mapping can be approximated by the linear map

$$\boldsymbol{Z}_{i+1}-\boldsymbol{Z}_*(\bar{a})=\mathbf{A}\left(\boldsymbol{Z}_i-\boldsymbol{Z}_*(\bar{a})\right)+\boldsymbol{B}(a-\bar{a}) \tag{22}$$

The partial derivatives $\mathbf{A}=\mathbf{D}_{\boldsymbol{Z}}\boldsymbol{F}(\boldsymbol{Z}, a)$ and $\boldsymbol{B}=\mathbf{D}_a\boldsymbol{F}(\boldsymbol{Z}, a)$ are evaluated at $\boldsymbol{Z}=\boldsymbol{Z}_*(\bar{a})$ and $a=\bar{a}$. The time-dependence of the parameter a is a linear function of variable $\boldsymbol{Z}_i$ of the form

$$a-\bar{a}=-\boldsymbol{K}^{\mathrm{T}}\left(\boldsymbol{Z}_i-\boldsymbol{Z}_*(\bar{a})\right) \tag{23}$$

Substituting (23) into (24)

$$\boldsymbol{Z}_{i+1}-\boldsymbol{Z}_*(\bar{a})=\left(\mathbf{A}-\boldsymbol{B}\boldsymbol{K}^{\mathrm{T}}\right)\left(\boldsymbol{Z}_i-\boldsymbol{Z}_*(\bar{a})\right) \tag{24}$$

As (24) shows that, if the matrix $\mathbf{A}$-$\boldsymbol{B}\boldsymbol{K}^{\mathrm{T}}$ is asymptotically stable (i.e. the modulus of the eigenvalues is less than 1), then the fixed point will be stable. The key problem is to determine the feedback matrix $\boldsymbol{K}^{\mathrm{T}}$, which satisfies the above condition. The literature [23] has given the method to calculate the pole placement. The pole placement problem has a unique solution if and only if the $n \times n$ matrix

$$\mathbf{C}=\left[\boldsymbol{B}\ \ \mathbf{A}\boldsymbol{B}\ \ \mathbf{A}^2\boldsymbol{B}\ \cdots\ \mathbf{A}^{n-1}\boldsymbol{B}\right] \tag{25}$$

The matrix's rank is n. ($\mathbf{C}_{n\times n}$ is called the controllability matrix). The solution of the pole placement problem is given by

$$\boldsymbol{K}^{\mathrm{T}} = \left[\alpha_n - a_n, \cdots, \alpha_1 - a_1\right]\mathbf{T}^{-1} \tag{26}$$

Where $\mathbf{T} = \mathbf{CW}$, and

$$\mathbf{W} = \begin{pmatrix} a_{n-1} & a_{n-2} & \ldots & a_1 & 1 \\ a_{n-2} & a_{n-3} & \ldots & 1 & 0 \\ \ldots & \ldots & \ldots & \ldots & \ldots \\ a_1 & 1 & \ldots & 0 & 0 \\ 1 & 0 & \ldots & 0 & 0 \end{pmatrix},$$

Here a_i (i=1,2…) are the coefficients of the characteristic polynomial of **A**, $\left|\lambda I - \mathbf{A}\right| = = \lambda^n + a_1\lambda^{n-1} + \cdots + a_n$, and $\alpha_1, \cdots, \alpha_n$ are the coefficients of the desired characteristic polynomial of $\mathbf{A}$-$\boldsymbol{BK}^{\mathrm{T}}$

$$\left|sI - \left(\mathbf{A} - \mathbf{B}\boldsymbol{K}^{\mathrm{T}}\right)\right| = s^n + \alpha_1 s^{n-1} + \cdots + \alpha_n.$$

After $\boldsymbol{K}^{\mathrm{T}}$ is determined by $\left|a - \bar{a}\right| < \delta$ and (23), we have

$$\left|\boldsymbol{K}^{\mathrm{T}}\left(\mathbf{Z}_i - \mathbf{Z}_*(\bar{a})\right)\right| < \delta.$$

We select the appropriate parameters to achieve the purpose of control.

6. Numerical Simulation

6.1 The projection of the Poincaré map

First, we take a set of parameters $\mu_m = 2, \mu_k = 5, f_2 = 0, R = 8, b = 1.5$. When ω=0.65, the eigenvalues of the linearized matrix are within the unit circle. The stable periodic motion shows a stable fixed point in the Poincaré projection, as shown in Figure 2. When ω= 0.743, a pair of complex conjugate eigenvalues of the linearization matrix, whose modulus is greater than 1. The impact vibration system occurs Hopf bifurcations. The attracting invariant circles appear in the Poincaré projection, as shown in Figure 3. A single torus doubling begins to occur as the value of as the value of ω passes through 0.7521, *as* shown in Fig. 4. When the value of ω increases further, the system will become chaotic motion, as shown in Fig. 5. Since there is a slight disturbance, the system appears chaotic, which reflecting the sensitivity of initial value and the uncertainty.

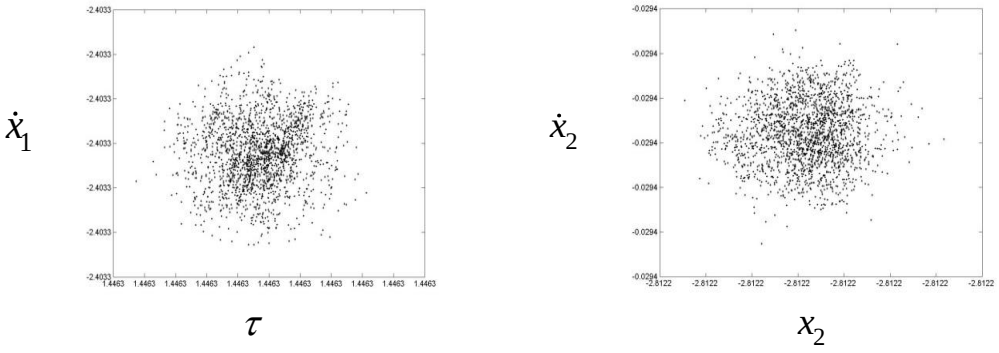

Fig. 2. The fixed points of the system shown in projected Poincaré sections

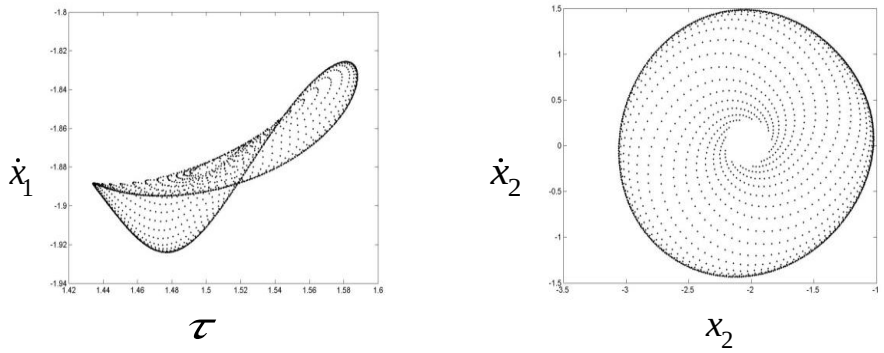

Fig. 3.The invariant circles of the system shown in projected Poincaré sections

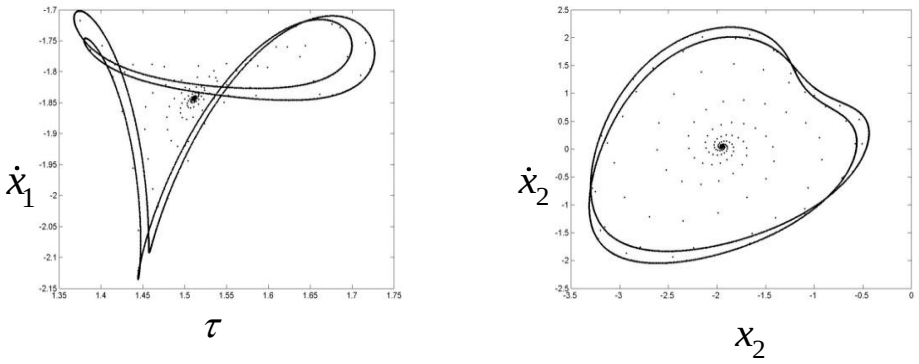

Fig. 4. The torus doubling of the system shown in projected Poincaré sections

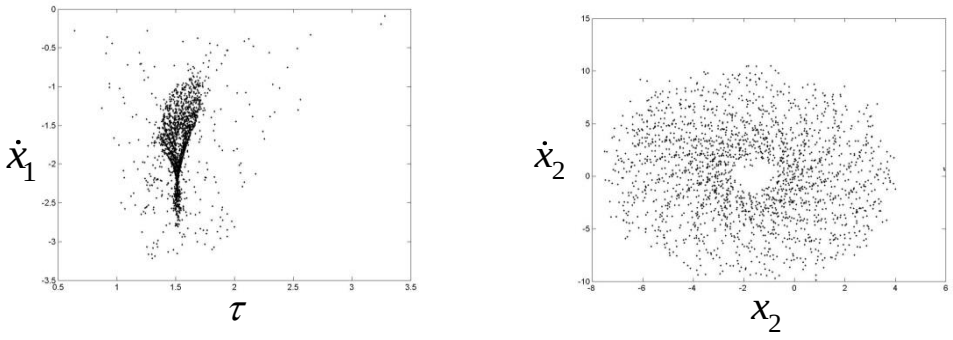

Fig.5.The chaotic motion of the system shown in projected Poincaré sections

6.2 Chaos Control of the vibro-impact system

Linearization of the Poincaré map, when $\omega = 0.7896$, the motion of the system is chaotic. ω is chosen as a control parameter. By computer the partial derivative. According to the method described above, based on the Poincaré map of a two-degree-of-freedom system, the mapping is linearized by the principles of linear approximation. The appropriate poles $k_i, (i = 1,2,3,4)$ and the disturbance δ are selected, and the controlled parameter of the system is perturbed continuously every moment. The unstable fixed point will move along the stable manifold after applying parameter perturbation. So again and again, the system is controlled to an unstable fixed point finally. The chaotic behavior of the two-degree-of-freedom vibro-impact system is controlled. The feasibility and the effectiveness of the theoretical analysis is verified by the numerical simulation.

We select the poles k_1, k_2 is 0 each, the other two poles k_3, k_4 are eigenvalues of the linearization matrix whose modes are less than 1. Let the perturbation δ be 0.02, after 5400 iteration times, the system is controlled on the fixed point (Periodic orbit), see Figure 6.

Let the perturbation δ be 0.03, after 1800 iteration times, the system is controlled on period-2, see Figure 7.

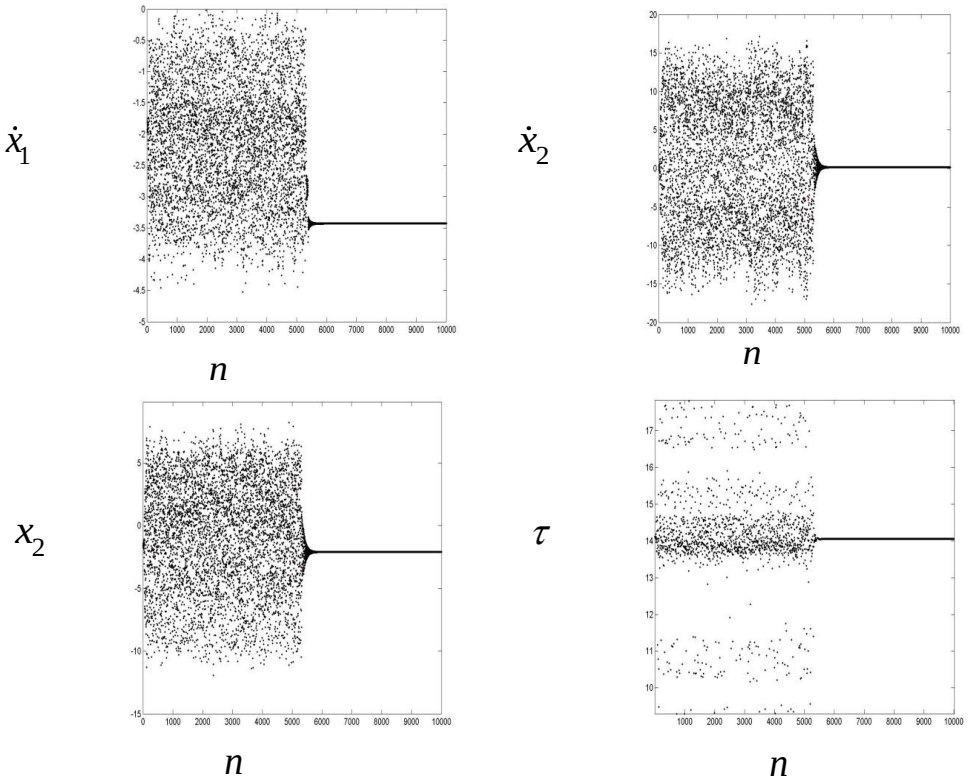

Fig. 6. Controlling of the period-1 orbit, δ=0.02

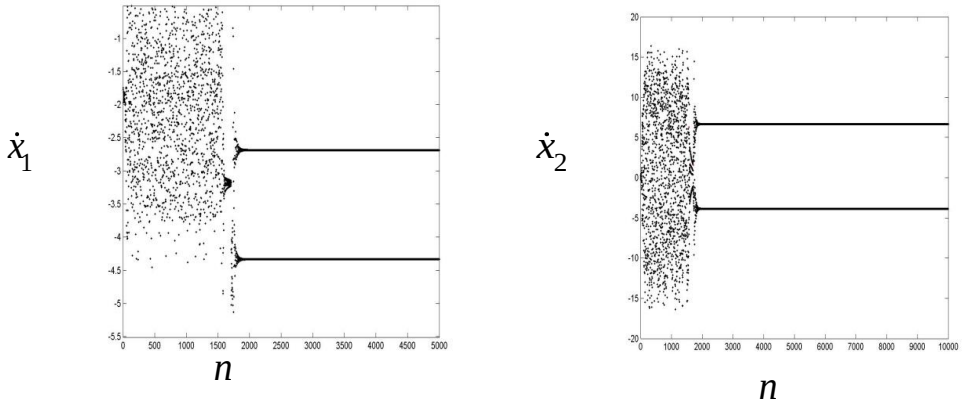

Fig. 7. Controlling of the period-2 orbit, δ=0.03

Let the perturbation δ be 0.05, 0.1 respectively, the system is controlled on periodic-2 after 500 and 100 iteration times. This indicates that the time of the complete chaos control is influenced by the different values of the perturbation δ greatly, see Fig. 8.

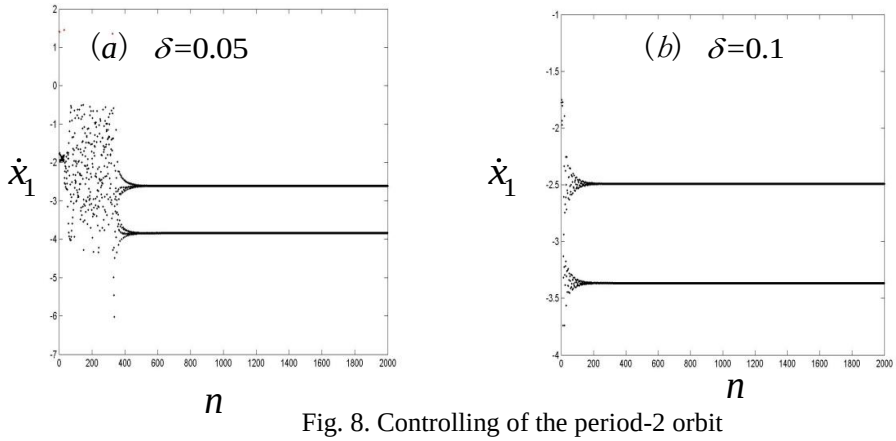

Fig. 8. Controlling of the period-2 orbit

We select the poles μ_1, μ_2 is 0.2, 0.1 each, the other two poles μ_3, μ_4 are the same with above values. The unstable fixed point $X^* = \left(\dot{x}_1^*, x_1^*, \dot{x}_2^*, \tau^*\right) = \left(-2.94, -2.18, -0.79, 37.17\right)$. Let the perturbation δ be 0.02, $\dot{x}_1$ is controlled on a regional belt between -2.94 and -2.88 and $\dot{x}_2$ is controlled on a regional belt between -0.86 and 1.12 after 5400 iteration times. The system cannot be controlled on the unstable fixed point accurately, as shown in Fig. 9.

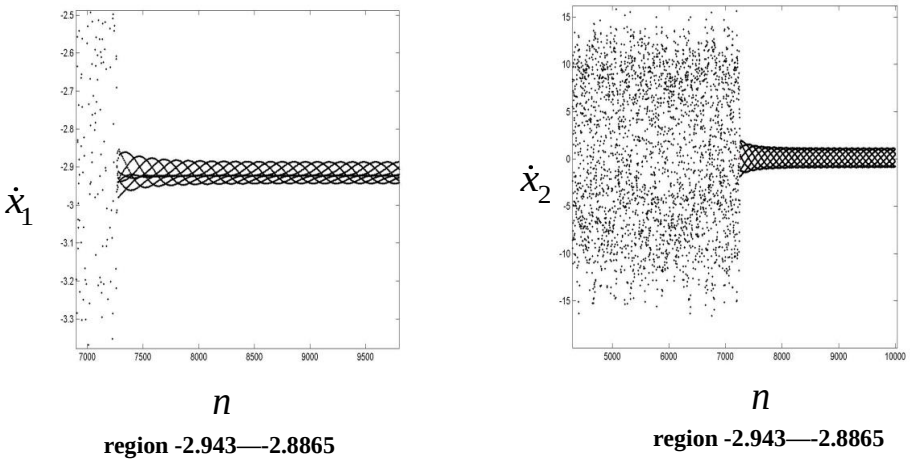

Fig. 9. Controlling to a region which contains of the fixed points

7. Conclusions

This paper studies the dynamic behavior of the vibro-impact system. At first the Poincaré cross-section is determined and Poincaré mapping is established. When the excitation frequency is different, a Hopf bifurcation will exist, even the

system will exhibit chaos phenomenon. Through the improvement of OGY and using the pole placement technique of the linear control theory, the chaotic motion of the vibro-impact system is controlled. At the same time, the different choice of the regulator poles is analyzed. The time of the complete control is influenced by the different of the disturbance and poles. The research results show that the OGY Chaos control method can be implemented in two or more degrees of freedom vibration system.

REFERENCES

[1]. *Kapitaniak T,* Chaotic oscillations in mechanical systems. Manchester University Press, (1991)

[2]. *Pfeiffer F., Glocker C,* Multibody dynamics with ucnilateral contats. John Wiley & Sons, (1996)

[3]. *Laggiard E., Runkel J,* One-dimensional bimodel of vibration and impacting of instrument tubes in a boiling water reactor. Nuclear Science and Engineering, (1993), 115: 62-70.

[4]. *Feng Q., Pfeiffer F.,* Stochastic model on a rattling system. Journal of Sound and Vibration, (2012), 215: 439-453.

[5]. *Luo G. W., Xie J. H.,* Hopf bifurcation of a two-degree-of-freedom vibro-impact system. Journal of Sound and Vibration, (2012), 213: 391-408.

[6]. *Xie J. H., Ding W. C.,* Hopf-Hopf bifurcation and invariant torus T^2 of a vibro-impact system. International Journal of Non-Linear Mechanics, (2013), 40: 531-543.

[7]. *Shaw. S. W., Holmes. P.J.,* A periodically forced piecewise linear oscilinear. Journal of Sound and Vibration, (1983), 90: 129-155.

[8]. *Blazejczyk-Okolewska B.,* Analysis of an impact damper of vibrations. Chaos, Solitons & Fractals, (2014), 12: 1983－1988.

[9]. *Yue Y., Xie J. H,* Symmetry of the Poincaré map and its influence on bifurcations in a vibro-impact system. Journal of Sound and Vibration, (2011), 323: 292-312.

[10]. *Luo G. W., Lv X. H,* Controlling bifurcation and chaos of a plastic impact oscillator. Nonlinear Analysis: Real World Applications, (2013), 10: 2047-2061.

[11]. *Ott E., Grebogi C., Yorke J. A.,* Controlling chaos. Phys. Rev. Lett., (1990), 64: 1196-1199.

[12]. *Pyragas K.,* Continuous control of chaos by self-controlling feedback. Phys. Lett. A, (1992), 170: 421-428.

[13]. *Shinbrot T., Grebogi C., Ott E.,* Using small perturbations to control chao. Nature, (1993), 363: 411-417.

[14]. *Pyragas K.,* Predictable chaos in slightly perturbed unpredictable chaotic systems. Phys. Lett. A, (1993), 181: 203-210.

[15]. *Boccaletti S, Grebogi C, Lai Y. C., Mancini H, Maza D.,* The control of chaos: theory and applications. Physical Reports, (2011), 329:103-197.

[16]. *Yagasaki K., Uozumi T.,* A new approach for controling chaotic dynamical systems. Phys. Lett. A, (1998), 238: 349-357.

[17]. *Yagasaki K., Uozumi T.,* Controlling chaos using nonlinear approximations and delay coordinate embedding. Phys. Lett. A, (2012), 247: 129-139.

[18]. *Auerbach D., Grebogi C., Ott E., Yorke, J. A.,* Controlling chaos in high dimensional systems. Phys. Rev. Lett., (2013), 69(24): 3479-3482.

[19]. *Boccaletti S., Grebogi C., Lai Y. C., Mancini H., Maza D.,* The control of chaos: theory and applications. Physical Reports, (2015), 329: 103-197.

[20]. *Flipe Romeiras J., Grebogi C., Ott E., Dayawansa.,* Controlling chaotic dynamical systems. Physica D, (2014), 58: 165-192.
[21]. *Souza de. SLT, Caldas I. L.,* Controlling chaotic orbits in mechanical systems with impacts. Chaos, Solitons and Fractals, (2014), 19: 171-178.
[22]. *Casas F, Grebogi C,* Control of chaotic impacts. International Journal of Bifurcation and Chaos, (2015), 7: 951-955.
[23]. *Ogata K,* Controlling Engineering. Prentice Hall, Englewood Cliffs, NJ, (1990), Second Ed: 782-784.